

Transmission Power Control in 2-D Wireless Sensor Networks Powered by Ambient Energy Harvesting

Hwee-Pink Tan^{*}, Alvin Valera^{*} and Wenbin Koh[†]

^{*}Networking Protocols Department, Institute for Infocomm Research (Singapore)

[†]Department of Electrical and Computer Engineering, National University of Singapore (Singapore)

Email: {hptan, acvalera}@i2r.a-star.edu.sg and kohwenbin@nus.edu.sg

Abstract—We are witnessing pervasive use of wireless sensor networks (WSNs) in a wide variety of applications such as monitoring of road infrastructure. As they are expected to be deployed in harsh environments for long durations, the research community have turned their attention to tapping on ambient energy to power such networks. However, since energy harvesting rates are still significantly lower than the power consumption in each wireless sensor node, the energy availability is sporadic, making the design of runtime policies in WSN powered by ambient energy harvesting (WSN-HEAP) to maximize performance an important but challenging task.

In this paper, using extensive simulations, we evaluate the efficacy of transmission power control for 2-D WSN-HEAP deployed in a grid topology in terms of throughput, data delivery ratio and fairness. When a fixed power is assigned to all nodes, we observe a trade-off between throughput and fairness: throughput is maximized at lower powers at the expense of fairness and vice versa. When nodes are assigned powers according to their proximity from the sinks, we observe that assigning the *minimum* transmission power required for each node to communicate with its nearest sink maximizes all performance metrics. This indicates that minimizing interference dominates over multi-sink redundancy in a 2-D WSN-HEAP.

I. INTRODUCTION

With the advancement in Micro-Electro-Mechanical Systems (MEMS) technology, we are witnessing the use of wireless sensor networks (WSNs) for a myriad of predictive monitoring applications such as road infrastructure monitoring [1]. Unlike event-driven monitoring applications (e.g., detection of threats and oil spills) where data dissemination is only triggered upon the detection of abnormal phenomena, sensed data is continuously being disseminated (e.g., periodically) in predictive monitoring. Hence, while maintaining high data reliability is of primary importance in event-driven monitoring, achieving high data throughput and fairness is also essential for predictive monitoring.

Since WSNs are expected to be deployed in harsh or inaccessible environments for long periods of time, the WSN research community have recently turned their attention to tapping on *ambient energy* such as solar, vibrational, wind and thermal energy to replace/supplement batteries to power WSNs. Since ambient energy is always available, such WSNs powered solely by ambient energy harvesting (which we refer to as WSN-HEAP in this paper) are more effective and economical in the long-term as they can remain operational for very long durations until hardware failure. However, since

energy harvesting rates vary with the environment and are still significantly lower than the power consumption in each wireless sensor node, the energy availability is sporadic, making the design of runtime policies to maximize performance an important but challenging task.

Most existing work in energy harvesting WSNs (e.g., [2]) assume that energy harvesting is used to supplement battery supply, and focus on adapting duty cycles and task scheduling by predicting future energy availability. Game theory is also applied to find the optimal parameters for a sleep and wakeup strategy to tradeoff between packet blocking and dropping probabilities [3]. However, the prediction of future energy availability is difficult in practice as empirical characterization of energy harvesting sensor nodes [4] have shown that the energy harvesting times do not *always* exhibit time correlation.

Alternatively, the power consumption profile can be adapted to fit the energy profile by tuning the transmission power on a per-node basis. In traditional battery-powered WSNs, this is widely used to maximize the network lifetime for a given offered load subject to total network power constraint [5]. In cellular networks, location-based power control schemes are proposed [6] for mobile devices where the transmission power of a device is continuously adjusted *temporally* according to its distance from the base station (sink).

Since WSN-HEAP are not subject to network power constraints and mobility, transmission power control can be used to adjust both the sending rate as well as reliability of packet delivery to maximize performance. In our previous work [7], we considered a linear WSN-HEAP for railroad health monitoring and investigated the data delivery performance when the transmission power assigned to each node is varied.

In this paper, we evaluate location-based transmission power control schemes for a 2-D WSN-HEAP deployed in regular grid topology for monitoring of road infrastructure. We show via extensive simulations that throughput, data reliability and fairness are maximized by assigning the *minimum* transmission power required for each node to communicate with its nearest sink.

We define our system model for a 2-D WSN-HEAP in Section II. We describe several location-based transmission power allocation schemes in Section III, and evaluate their impact on the performance of a 2-D WSN-HEAP in Section IV. Finally, we provide some concluding remarks and directions for future research in Section V.

II. SYSTEM MODEL

In this section, we present our system model for WSN-HEAP, which is motivated by existing commercial-off-the-shelf energy harvesting sensor motes such as Ambio24 [8], which (i) functions with solar and vibrational energy harvesters, (ii) operates in a single-hop architecture, i.e., it can only be configured either as a source or a sink, and (iii) transmits sensed data as soon as sufficient energy is harvested.

A. Energy and Traffic Model

Each WSN-HEAP node comprises various components as illustrated in Figure 1. The energy harvesting device converts ambient energy into electrical energy which is cumulatively stored in the energy buffer (e.g., in supercapacitors), while the node is *idle*. This is because the achievable harvesting rates today are still significantly lower than the power consumption of the other components.

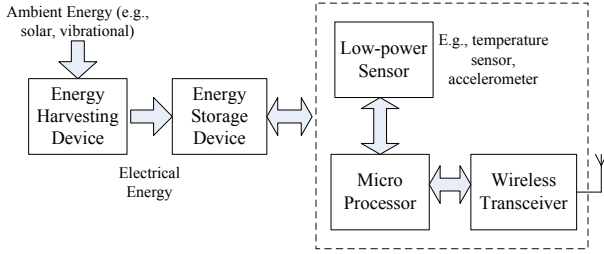


Fig. 1. Components of a WSN-HEAP device.

Once the stored energy reaches a useful level, E_f (J), the microprocessor will actuate the low-power sensor, and the sensed data is transmitted as a packet (s_d bits) to the sink(s) at α bps, while energy is still being harvested. The above is repeated when the stored energy reaches an unusable level, as shown in Figure 2.

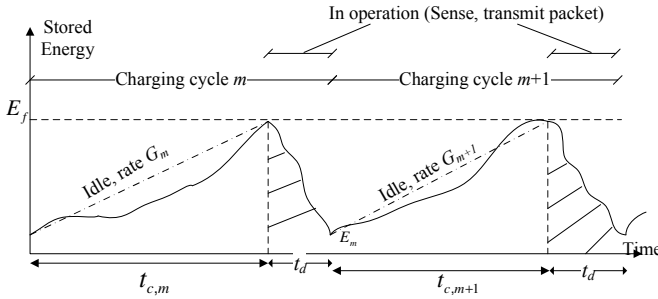


Fig. 2. Energy model of a WSN-HEAP device.

Assuming that the microprocessor and transceiver constitute the main power consumers (consuming P_μ and P_δ W respectively) in each WSN-HEAP node [9], the energy expended during transmission of a data packet of duration $t_d = \frac{s_d}{\alpha}$ is $(P_\delta + P_\mu)t_d$. To ensure that there is sufficient stored energy in each cycle to transmit a packet, we set $E_f = (P_\delta + P_\mu)t_d$.

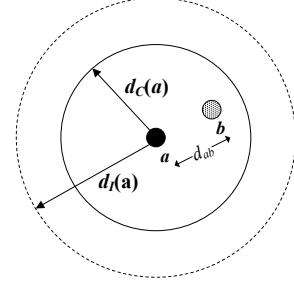


Fig. 3. Illustration of communication ($d_C(a)$) and interference ($d_I(a)$) range for node a .

B. Propagation Model

We assume a simple free-space direct-ray path-loss model, where, given transmission power of P_a from node a , the received signal strength, P_{rec} , at a distance d away can be evaluated as follows:

$$P_{rec} = \frac{K P_a}{d^\gamma}, \quad (1)$$

where the propagation factor, K , depends on the antenna gain and some reference distance, and γ is the path-loss exponent that depends on the carrier frequency and the environment.

Node a 's transmission can be correctly decoded at node b if its received signal strength exceeds the receiver sensitivity, denoted by \tilde{P}_s . Accordingly, we define the *communication* range of node a , $d_C(a)$, as follows:

$$d_C(a) = \left(\frac{K P_a}{\tilde{P}_s} \right)^{\frac{1}{\gamma}}. \quad (2)$$

On the other hand, node a 's transmission will be detected (but not correctly decoded) at (and hence, potentially interfere with an intended transmission to) node b , if its receive signal strength at node b exceeds the propagation limit, denoted by \tilde{P}_l , but falls below \tilde{P}_s , where $\tilde{P}_l < \tilde{P}_s$. Accordingly, we define the *interference* range of each potentially interfering node t , $d_I(t)$, as follows:

$$d_I(t) = \left(\frac{K P_t}{\tilde{P}_l} \right)^{\frac{1}{\gamma}}. \quad (3)$$

This is illustrated in Figure 3. Accordingly, node a 's transmission can be correctly decoded at node b at distance d_{ab} away if the Signal-to-Interference Ratio (SINR) exceeds a certain threshold, θ , where:

$$SINR = 10 \log_{10} \frac{\frac{K P_a}{d_{ab}^\gamma}}{P_{noise} + \sum_{j: d_{jb} \leq d_I(j)} \frac{K P_j}{d_{jb}^\gamma}},$$

and P_{noise} is the receiver noise power.

C. Deployment Topology

WSN-HEAP can be deployed in many road infrastructure monitoring applications where ambient energy sources are available. A possible application is in the monitoring of bridge frost during winter, where the vibration of the bridge can be harvested to power wireless sensor nodes. The formation of road or bridge frost depends primarily on the pavement temperature and dew point temperature. A real-time, accurate “picture” of the pavement surface temperature and the corresponding dew point temperature on sensitive sections of the road or bridge network is useful to provide information for decision makers to plan anti-icing operations prior to manpower or materials dispatch and before surface temperatures reach the freezing point. This can be achieved by installing wireless sensors at regular intervals and a few mains-powered sinks to relay the information.

For this paper, we deploy 16 such sinks in a 4 x 4 regular grid, with grid size of $x \times x$ metres. WSN-HEAP nodes are then deployed uniformly (with known locations obtained from GPS during deployment) with n nodes in between each sink and its nearest neighboring sink. An illustration for the case of $n = 2$ is given in Figure 4.

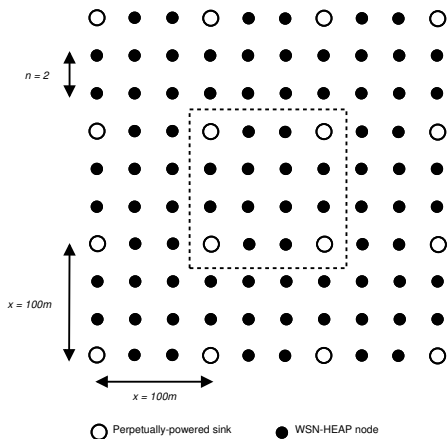


Fig. 4. Two-dimensional grid deployment of WSN-HEAP nodes and sinks. The area inside the dotted box is the region of interest (ROI).

III. TRANSMISSION POWER CONTROL SCHEMES

In this paper, we consider transmit power control as a means to maximise throughput, reliability and fairness in a 2-D WSN-HEAP. The simplest power allocation scheme is to assign the *same* (fixed) transmit power to all nodes (**FP**). A large transmit power permits direct communication with more sink(s) (multi-sink redundancy) but reduces the offered load (longer harvesting period) and introduces the near-far effect. On the other hand, assigning low transmit powers would increase the offered load and reduce the level of interference, at the expense of reducing the scope for exploiting multi-sink redundancy.

However, since nodes have different (but known) proximity to the sinks, intuitively, they should be assigned transmit

powers accordingly so as to balance the inherent trade-offs between (high offered load, low interference) with multi-sink redundancy with the **FP** scheme. Based on Eqn. (2), the transmit power needed to reach a communication range of x , $P(x)$, is given by:

$$P(x) = \frac{\tilde{P}_s}{K} x^\gamma. \quad (4)$$

Hence, each node can compute the transmission power required to communicate with, or interfere with other transmissions at, the sink(s). Let $d_{min,i,j}$ be the distance from node i to its j nearest sink(s).

Accordingly, we propose the following *location-based* power allocation schemes:

- **Minimum-Interference Allocation (MI)** To minimise the near-far effect, node i sets its transmit power, P_i , such that it only reaches its nearest sink, i.e.,

$$P_i = P(d_{min,i,1}).$$

- **Multi-Sink Allocation (MS(j))** To maximise the scope of multi-sink redundancy, node i sets its transmit power, P_i , such that it can communicate with j of its nearest sinks, $j \geq 2$, i.e.,

$$P_i = P(d_{min,i,j}).$$

Although the communication range of some nodes may span beyond the sinks, their impact is only manifested at the sinks since WSN-HEAP nodes do not “receive”.

Figure 5 shows an example of these location-based power control schemes for one specific node.

IV. SIMULATION RESULTS

We evaluate the performance of a 2-D WSN-HEAP for condition monitoring of road infrastructures based on simulation results obtained using the Qualnet [10] network simulator.

The power consumption parameters are obtained from the specifications of commercially available MICAz sensor motes [11], with an operating voltage of 3V. Based on the data sheet of the CC2420 radio, we perform a polynomial fit to obtain the approximate relationship between transceiver power dissipation during packet transmission, P_δ and the corresponding transmission power, P_t as shown in Figure 6(a). The parameters used are summarised in Figure 6(b).

The propagation factor, K , is computed using Eqn. (2) based on a communication range of 100m at maximum transmit power of 1mW (0 dBm). We also set x to the communication range to allow multi-sink redundancy to be exploited. We consider an SINR threshold of 7 dB and assume a mean charging rate, $E[G] = 0.5\text{mW}$ for all nodes. The deployment density considered in this study ranges from $n=1$ to 8.

To eliminate edge effects, we define a region of interest (ROI) comprising $N = 4n+n^2$ WSN-HEAP nodes and 4 sinks (c.f. Figure 4) and only consider the packets transmitted and received within this region – WSN-HEAP nodes outside this region only contribute to interference at sinks.

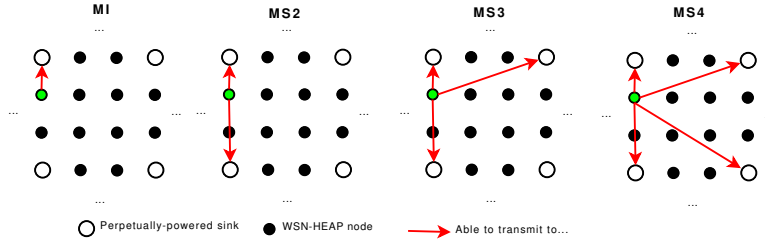


Fig. 5. Illustration of various location-based power control schemes.

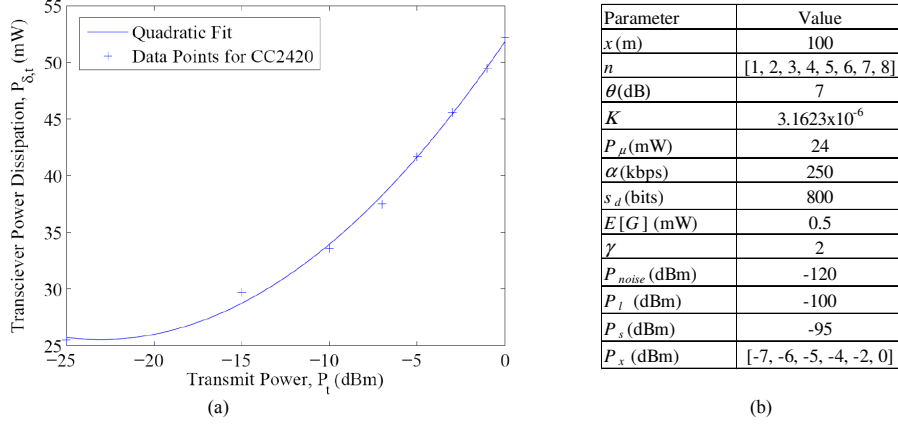


Fig. 6. (a) Transceiver power dissipation during packet transmission, P_{δ_t} (mW) vs transmit power, P_t (dBm) obtained with polynomial fit of CC2420 radio data and (b) Parameters for numerical results.

Let $p_{s,i}$ and $p_{r,i}$ be the total number of packets sent by node $i \in ROI$ and unique packets received at the sinks respectively over the simulation duration T . Node i 's throughput, R_i , is then given by:

$$R_i = \frac{p_{r,i}}{T}.$$

Hence, the network throughput density, S , is given by:

$$S = \frac{\sum_{i \in ROI} R_i}{x^2}.$$

Each packet from each WSN-HEAP node is successfully delivered as long as it arrives at *at least* one sink. Hence, the data delivery ratio for node i , DDR_i is given by:

$$DDR_i = \frac{p_{r,i}}{p_{s,i}}.$$

The average data delivery ratio, DDR , is then simply:

$$DDR = \frac{\sum_{i \in ROI} DDR_i}{N}.$$

Finally, by using Jain's fairness index [12], the overall network throughput fairness, F , is given by:

$$F = \frac{(\sum_{i \in ROI} R_i)^2}{N \sum_{i \in ROI} R_i^2}.$$

A. Fixed Power Comparison

We begin by first investigating the effect of assigning a fixed power for all WSN-HEAP nodes. We plot each performance metric as a function of deployment density for $FP(P_{FP})$ for various $P_{FP} \in [-7, -6, -5, -4, -2, 0]$ dBm in Figure 7.

1) *Throughput*: For each power, there is an optimal throughput which can be observed at different node densities. Prior to the optimal point, the throughput shows consistent increase, indicating that the additional packets generated by the added nodes can be accommodated by the network. After the optimal point, further increase in the number of nodes decreases the throughput which means that the additional traffic causes severe contention. The density at which the throughput reaches its peak depends on the transmit power. From 0 to -4 dBm, the throughput peaks at $n = 4$, while at -5 and -6 dBm, the throughput peaks at $n = 5$. At the lowest transmit power of -7 dBm, the throughput reaches the peak at $n = 6$. A more important observation is that at lower transmit power, peak throughput is higher compared to higher transmit power. At 0 dBm, peak throughput is 0.0024 packets/sec/m² while at -6 and -7 dBm, peak throughput is 0.0034 packets/sec/m². This result can be explained by the fact that when transmit power is low, the interference level is also low and therefore more nodes can be accommodated by the network before severe contention kicks in. Whereas when the transmit power is high, the interference level is also high, and the addition of fewer nodes can already cause

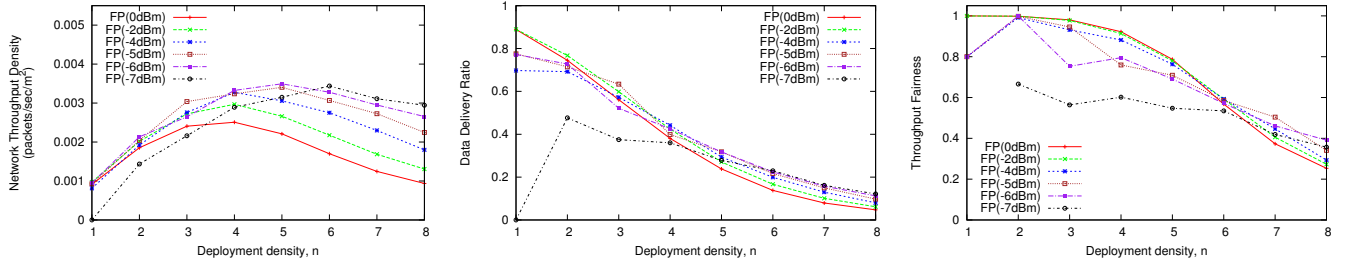


Fig. 7. Comparison of network throughput density (left), data delivery ratio (centre) and throughput fairness (right) obtained with FP scheme ($\theta = 7dB$)

severe contention. Hence, using low transmit power enables the deployment of more nodes which in turn leads to more packets being generated resulting in higher throughput density.

2) *Data Delivery Ratio*: For all the transmit powers evaluated, the data delivery ratio decreases with increasing deployment density. Note that at -7 dBm, the delivery ratio at $n = 1$ is 0 due to the fact that -7 dBm is not sufficient for all of the nodes to reach any of the sinks (at $n = 1$, minimum transmit power required is -6 dBm). Since the packet generation rate of all the nodes are roughly the same, higher deployment density entails higher overall packet generation rate. The decrease in DDR can therefore be attributed to increased level of contention due to the higher packet generation rate at higher node densities. There is essentially no clear winner in terms of DDR as the difference among the transmit powers are not significant except for -7 dBm which shows significantly low DDR at low deployment densities.

3) *Fairness*: Similar to DDR, fairness also shows a decrease as deployment density is increased for all transmit powers. This is because at higher node densities, contention becomes more severe resulting in nodes closer to the sink becoming more favored (near-far problem). In terms of transmit power, the higher transmit powers of 0 and -2 dBm consistently show the best fairness up to node density $n = 5$. This is expected since the use of high transmit power enables distant nodes in the network to deliver their packets to sinks. This may not be true at lower transmit power where only nodes physically closer to the sinks are more likely to deliver their packets. To clarify this point, we compute the required transmit power of nodes at the center of the ROI. Using Eqn. (4), we can calculate the required transmit power of a node at the center of the ROI (which is $50\sqrt{2}$ meters from any of the sinks):

$$\begin{aligned}
 P_{dBm}(x) &= 10 \log P(x) \\
 &= 10 \log \tilde{P}_s + 10 \log x^\gamma - 10 \log K \\
 &= -95 + 20 \log(50\sqrt{2}) - 10 \log(.0000031623) \\
 &= -95 + 37 + 55 = -3
 \end{aligned}$$

This means that a node at that location requires at least -3 dBm. Clearly, for transmit powers less than or equal to -4 dBm, nodes close to the middle of the ROI have no chance of having their packets reach the destination.

In summary, we observe a trade-off between network throughput density and fairness when assigning transmit power with the FP scheme: assigning high power maximizes fairness at the expense of throughput and vice versa. As such, for the rest of the study, 0 dBm (best in fairness) and -6dB (best in throughput) will be used for comparison against location-based schemes.

B. Comparison of Power Control Schemes

We now compare the performance of the fixed power scheme along with the different dynamic power control schemes. We plot each performance metric versus deployment density for various power control schemes in Figure 8.

1) *Throughput*: For each scheme, there is an optimal throughput which can be observed at different node densities. For the MS schemes, peak throughput is obtained at $n = 4$. For the MI scheme which shows the best throughput performance, peak throughput of 0.0042 packets/sec/m² is attained at $n = 5$. The underlying reason behind the superior performance of MI is that it enables greater spatial reuse. By transmitting only to the nearest sink, the MI scheme enables more nodes (at different locations) to have successful simultaneous transmissions. One interesting observation is that the fixed power scheme (-6 dBm) provides the best throughput at higher node densities ($n > 6$). One main difference between FP(-6 dBm) and MI is that in the latter, all nodes use -6 dBm transmit power regardless of their location¹. Whereas in the former, the farthest nodes from the sink located in the middle of the ROI use transmit power of around -3 dBm which is greater than -6 dBm. The worse performance of MI at $n > 6$ can therefore be attributed to the increased interference caused by these nodes. It is quite surprising that the MS schemes did not perform well in the simulations. In fact, MS(2) and MS(3) are only slightly better than FP(0 dBm) while MS(4) does not show any improvement over FP(0 dBm). This is due to the fact that the transmit powers allocated by these schemes are in the -2 to 0 dBm. Note that the throughput of MS(2) is comparable to that of FP(-2 dBm) while the throughput of MS(3) is in between FP(-2 dBm) and FP(0 dBm).

¹Note however that at transmit power of -6 dBm, nodes in the middle section of the ROI does not really reach any of the sinks. This partly explains the low fairness of FP(-6 dBm) compared to MI.

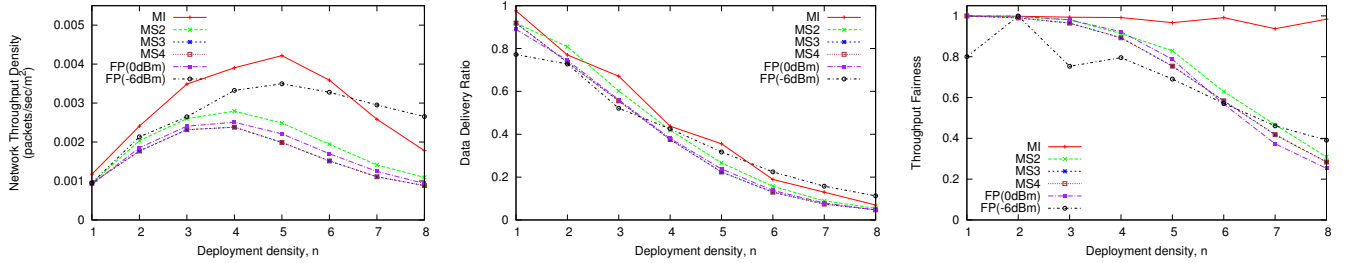


Fig. 8. Comparison of network throughput density (left), data delivery ratio (centre) and throughput fairness (right) obtained with various schemes ($\theta = 7dB$)

2) *Data Delivery Ratio*: For all the schemes, it can be observed that data delivery ratio decreases with increasing deployment density. As mentioned, this decrease is due mainly to the increased contention as the number of nodes is increased in the network. Similar to the DDR in **FP**, there is no clear winner in terms of the DDR as the difference among the different schemes are not significant. We expected the **MS** schemes to provide higher DDR as packets can reach multiple sinks. However, the impact of interference seems to outweigh the potential benefit of multi-sink redundancy.

3) *Fairness*: Except for **MI**, the fairness of all the other schemes decreases as the deployment density increases due to near-far problem where nodes closer to the sink become more favored. The **MI** scheme, which shows the best performance, maintained a fairness value close to 1 at all node densities. This is possible because **MI**'s low interference level enables the reception of data packets even from farther nodes. Recall that with the capture effect (SINR), when the interference level is low, there is a higher probability of decoding packets correctly even when the received power is low.

V. CONCLUSIONS

As wireless sensor networks are expected to be deployed in harsh environments for long durations, the research community have turned their attention to tapping on ambient energy as an alternative source to batteries to power such networks. However, since energy harvesting rates are still significantly lower than the power consumption, the energy availability is sporadic, making the design of runtime policies to maximize performance in Wireless Sensor Networks Powered by Ambient Energy Harvesting (WSN-HEAP) an important but challenging task.

We consider a 2-D WSN-HEAP for monitoring of bridge frost that comprises ac-powered sinks deployed in a regular grid, with WSN-HEAP nodes deployed uniformly amongst the sinks. Vibration energy generated from passing traffic is used to power the nodes, such that a data packet is sent directly to the sink(s) whenever sufficient energy is accumulated. We consider a fixed power scheme **FP**(P) where every node is assigned the *same* power, P , and a multi-sink scheme **MS**(j), where each node is assigned a power level just sufficient to communicate with its nearest j sinks. We denote by **MI** the special case where $j = 1$, since this scheme minimizes the interference while ensuring connectedness. We evaluate the

efficacy of these schemes in terms of throughput, data delivery ratio and fairness using simulations for various node densities.

For **FP**(P), we observe that there is an optimal density, n^* , that maximizes the throughput, where n^* is reduced as P is increased. Further, there is a trade-off between throughput and fairness: throughput is maximized at lower powers at the expense of fairness and vice versa. When compared against the **MS** and **MI** schemes, we observe that the **MI** scheme maximizes both throughput and fairness for all node densities. This indicates that the impact of interference seems to outweigh the potential benefits of multi-sink redundancy.

For future work, we plan to extend the evaluation to more realistic scenarios where energy harvesting rates vary temporally as well as spatially.

REFERENCES

- [1] J. Iaquina, "Use of micro-electro-mechanical systems and wireless sensor networks on road infrastructures," Transport Research Laboratory, Tech Report PPR 441, December 2008.
- [2] C. M. Vigorito, D. Ganesan, and A. G. Barto, "Adaptive control of duty cycling in energy harvesting wireless sensor networks," *Proc. of the IEEE SECON*, pp. 21–30, June 2007.
- [3] D. Niyato, E. Hossain, M. M. Rashid, and V. K. Bhargava, "Wireless sensor networks with energy harvesting technologies: A game theoretic approach to optimal energy management," *IEEE Wireless Communications*, vol. 14, no. 4, pp. 90–96, August 2007.
- [4] Z. A. Eu, H. P. Tan, and W. K. G. Seah, "Wireless Sensor Networks Powered by Ambient Energy Harvesting - An Empirical Characterization," *Accepted for Publication at IEEE ICC*, May 2010.
- [5] M. Kubisch, H. Karl, A. Wolisz, L. Zhong, and J. Rabaey, "Distributed Algorithms for Transmission Power Control in Wireless Sensor Networks," *Proc. of the IEEE WCNC*, pp. 558–563, March 2003.
- [6] P. N. Pathirana, "Location based Power Control for Mobile Devices in a Cellular Network," *Proc. of the IEEE TENCON*, pp. 1–6, November 2005.
- [7] H. P. Tan, W. Q. Lee, Z. A. Eu, and W. K. G. Seah, "Impact of Power Control in Wireless Sensor Networks Powered by Ambient Energy Harvesting for Railroad Health Monitoring," *Proc. of the IEEE AASNET*, May 2009.
- [8] "AmbioMote24 sensor mote specifications," available from <http://www.ambiosystems.com>.
- [9] G. V. Merrett, A. S. Weddell, A. P. Lewis, N. R. Harris, B. M. Al-Hashimi, and N. M. White, "An Empirical Energy Model for Supercapacitor Powered Wireless Sensor Nodes," *Proc. of the IEEE ICCCN*, August 2008.
- [10] "Qualnet 4.5, programmer's guide," *Scalable Network Technologies Inc*, <http://www.scalable-networks.com>.
- [11] "MICAz sensor mote specifications," available from <http://www.xbow.com>.
- [12] R. Jain, D. M. Chiu, and W. Hawe, "A quantitative measure of fairness and discrimination for resource allocation in shared computer system," Digital Equipment Corp., Tech Report DEC-TR-301, September 1984, available at <http://www.cs.wustl.edu/~jain/papers/fairness.htm>.